THE IMPORTANCE OF SURVEY APERTURE FOR IMAGING HIGH-TEMPERATURE GEOTHERMAL SYSTEMS WITH MAGNETOTELLURICS

Edward A. Bertrand[1], T. Grant Caldwell[1] and Fabian Sepulveda[2]

[1]GNS Science, 1 Fairway Drive, Avalon, Lower Hutt 5010, New Zealand

[2] Contact Energy, Wairakei Power Station, State Highway 1, Private Bag 2001, Taupo 3352, New Zealand

t.bertrand@gns.cri.nz

Keywords: *Magnetotellurics, Ohaaki, Taupo Volcanic Zone, Survey Design.*

ABSTRACT

Geothermal exploration of high-temperature geothermal systems commonly includes broadband magnetotelluric (MT) measurements, which can be sensitive to subsurface electrical resistivity structures at depths of 10 km or more. At shallow levels (~1-3 km depth), models of these MT data generally image a low-resistivity 'cap' (associated with hydrothermal brines and clays) embedded in a more resistive background. At greater depths (3 – 10 km), recent regional MT resistivity models (developed as part of GNS Science's Deep Geothermal Research Program in the southeastern Taupo Volcanic Zone) have revealed vertical low-resistivity anomalies (plumes) that may indicate the locations of deep upflows.

These low-resistivity 'plumes' are key to refining conceptual models of geothermal systems. However, the process of inversion modeling (in 2D and 3D) requires that surface measurements cover a spatial extent that is at least twice the intended depth of investigation. With interest increasingly shifting to deep (i.e. > 3 km depth) exploration, we use an existing industry-acquired MT survey of the Ohaaki geothermal field as a case study to assess: 1) suitability of the industry MT survey for imaging resistivity structures at depths greater than 3 km; 2) potential limitations associated with the relatively short recording time (overnight nominal) of the industry MT survey compared with the two-night recording time used for the regional MT survey.

By generating a series of 2D MT inversion models, we show that only when the regional MT data are added to extend the aperture of the industry MT survey, is the deep resistivity structure reliably resolved. We also show that while a single-night recording time does not preclude imaging the deep structure, the data quality can be noticeably improved with two-night recording. The lessons from this work are equally applicable to any geothermal system where MT surveys exist with limited spatial aperture.

1. INTRODUCTION

The Ohaaki geothermal system is located near the southeastern margin of the Taupo Volcanic Zone (TVZ), a young rifted-arc (Wilson et al., 1995) that contains more than 20 liquid-dominated geothermal systems (Bibby et al., 1995). Discovery of the Ohaaki geothermal field resulted from electrical resistivity surveys made during the 1950's and 60's (summarized in Hunt, 1989). These resistivity surveys indicated a single large geothermal system, which was later confirmed by drilling, and established Ohaaki as a type-locality to test geophysical methods for geothermal exploration. Numerous geophysical studies have since been carried out (e.g. Hochstein and Hunt, 1970; Risk et al., 1970; 1977; Risk, 1981; Henrys and van Dijck, 1987; Ingham, 1989; Risk, 1993), which include the following magnetotelluric surveys.

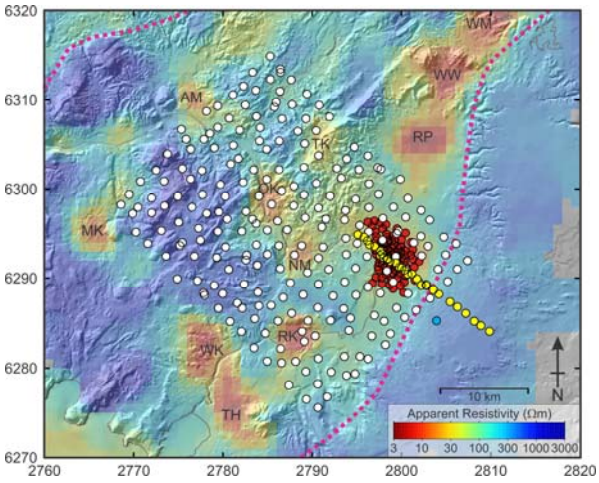

Figure 1: Map (in NZMG coordinate system) showing the locations of MT datasets in the southeast TVZ (yellow – GNS Science 2008; red – Contact Energy 2010; white – GNS Science 2010-2012 'deep geothermal'). The blue circle shows the GNS Science remote reference, the Contact Energy remote reference was located northeast of the map area. The background digital elevation model is overlain by the DC apparent resistivity map (Bibby et al., 1995) that correlates low resistivity zones to geothermal systems: TH – Tauhara, WK – Wairakei, RK – Rotokawa, MK – Mokai, NM – Ngatamariki, OK - Orakei Korako, OH - Ohaaki, TK – Te Kopia, AM – Atiamuri, RP – Reporoa, WW – Waiotapu Waikiti, and WM – Waimangu. The pink dashed lines show the boundaries of the TVZ after Wilson et al. (1995). (Map modified from Bertrand et al., 2012).

In 2008, GNS Science measured MT data at 42 sites along a ~NW-SE profile that transects the Ohaaki geothermal field (yellow circles in Figure 1). Data were recorded for 2 night's duration using Phoenix Geophysics Ltd. MTU systems. A remote reference site was operated on the Kaingaroa Plateau (blue circle in Figure 1), and these data were robust processed using the Phoenix SSMT 2000 code.

In summer 2010, an MT survey of Ohaaki was conducted by Schlumberger Seaco Inc. (WesternGeco) for Contact Energy. In total, data were recorded at 89 MT sites for 1

night's duration using Metronix ADU-06 receivers (red circles in Figure 1). A remote reference site was located northeast of the survey area on the Kaingaroa Plateau. Further details on this survey can be found in SKM (2011).

During 2010-2012, GNS Science collected an additional 220 MT measurements that form a regional array in the southeast Taupo Volcanic Zone (white circles in Figure 1; Bertrand et al., 2012). MT data at these sites were also measured for 2 night's duration using Phoenix Geophysics Ltd. MTU systems and processed using SSMT 2000.

2. ASSESSMENT OF DATA QUALITY

Underpinning any geophysical inversion model is the observational data upon which it is based. This fact is particularly true in MT geothermal exploration, where data in the period range 1 – 10 s is often crucial for determining the depth to the conductor-resistor boundary, often associated with the transition from low- to high-temperature alteration. Unfortunately, this period range overlaps with the so-called 'dead-band' where the natural MT signals are weak and high-quality data are hard to obtain (see Appendix-I). In some areas near the Ohaaki geothermal field, intense dairy farming is carried out using numerous electric fences and exacerbates this situation further. If not turned-off during MT data acquisition, these electric fences can severely degrade the quality of the measured data.

Despite these difficulties, all of the MT data used in this study (acquired by WesternGeco and GNS Science) are in general, of good quality. Figure 2 shows 4 pairs of sites collected by WesternGeco and GNS Science that are located nearby each other, and used for a side-by-side comparison of the unedited MT sounding curves (Figures 3 and 4). Overall, these pairs of sounding curves are similar in shape, as they should be for nearby measurements that have not been distorted by near-surface structure present at one site but not the other. However, in general, the GNS Science curves (right panels in Figures 3 and 4), especially the phase, are smoother than the corresponding WesternGeco curves (left panels in Figures 3 and 4).

The data compared in Figures 3 and 4 were acquired at different times and some variations observed, particularly at short periods (i.e. ~<0.1s), may be due to the strength of the electromagnetic noise field during recording. At longer periods, a significant difference between these MT surveys is the length of time that data is acquired at each site; GNS Science record for 2 night's duration compared to 1 night's duration for WesternGeco. Although many factors combine to influence final MT data quality (including the strength of the natural source fields at the time of acquisition, see Appendix-I), the consistent improvement in data quality at the sites shown in Figures 3 and 4 may be a direct result of the increased recording time used by GNS Science. Recording time-series data for 2 night's duration (~40 hours) has the following advantages:

- longer recording improves the signal-to-noise ratio,
- and provides an increased chance of measuring time-series data during a period of low noise and high signal strength, which can be identified during cross-power editing.

However, in spite of the potential improvements in data quality using extended acquisition time, logistical advantages may result from reduced acquisition time. Depending on the goals of the MT survey, and the number of instruments available, overnight recording time can be a practical choice.

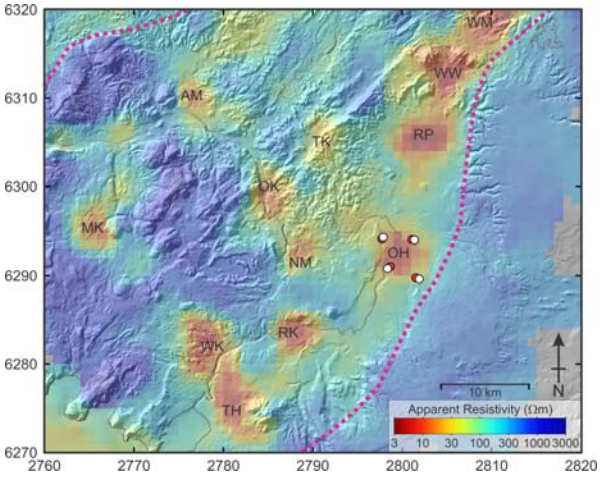

Figure 2: Map (in NZMG coordinate system) showing the locations of nearby GNS Science MT data (white circles) and Contact Energy MT data (red circles) used in the side-by-side comparisons shown in Figures 3 and 4. All other labels as in Figure 1.

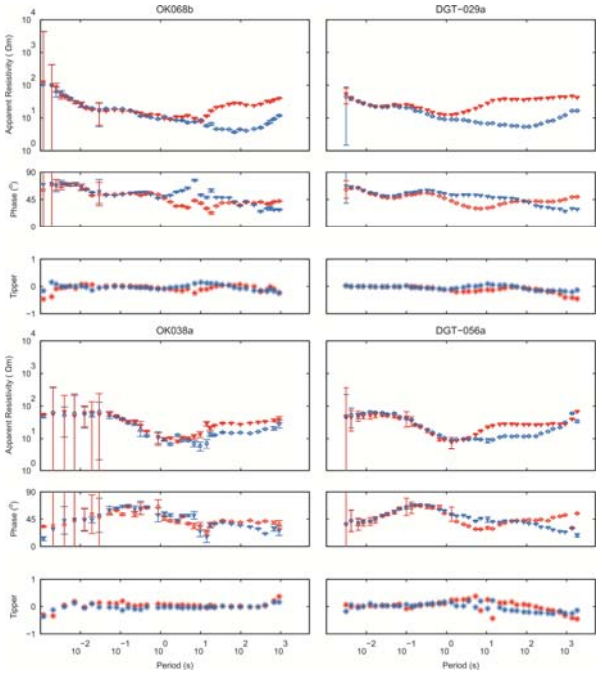

Figure 3: MT Sounding curves (rotated to 0°N) for pairs of sites at nearby locations (Figure 3). The left panels show Contact Energy measurements, and the right panels show corresponding GNS Science measurements.

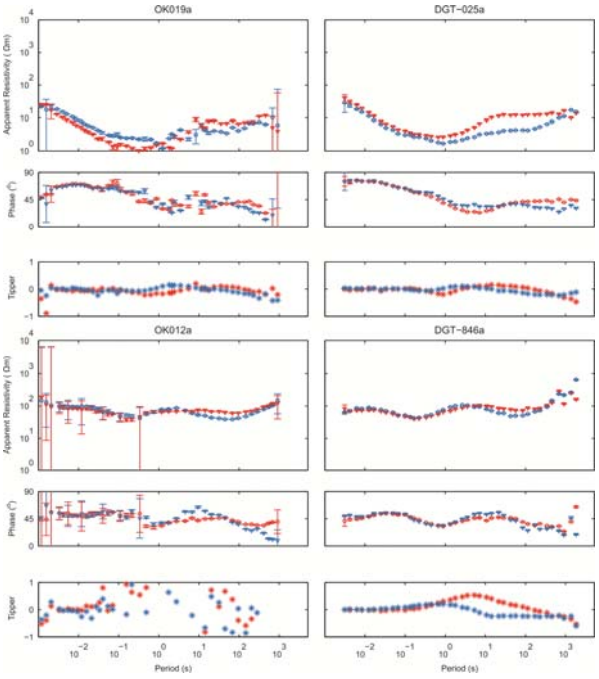

Figure 4: MT Sounding curves (rotated to 0°N) for pairs of sites at nearby locations (Figure 3). The left panels show Contact Energy measurements, and the right panels show corresponding GNS Science measurements.

3. INVERSION SETTINGS AND CONTROL PARAMETERS

To investigate survey design and data characteristics required to reliably image resistivity structure at depths down to 7 km beneath the Ohaaki geothermal field, a series of 2D inversion models were generated using the NLCG6 algorithm (Rodi and Mackie, 2001) contained within the WinGLink software package. A total of three inversion models were generated using:

a. only Contact Energy MT data,

b. a combination of Contact Energy and GNS Science MT data, and

c. using only GNS Science MT data.

In order for comparisons between these resistivity inversion models to yield insight into data characteristics and survey design alone, each inversion model was generated using an identical set of electromagnetic field polarizations (or modes), discretization grids and inversion control parameters that include:

- TE and TM mode impedance data were inverted between the period range 0.01 to 300 s. In order to facilitate combining the Contact Energy and GNS Science MT data, both datasets were interpolated to a set of regular periods (8 per decade).

- The inversion algorithm was set to solve for the smoothest model, using a standard grid Laplacian operator and to minimize the model Laplacian.

- Tau, the regularisation parameter that balances the trade-off between fitting the data and generating a smooth model was set to 3. Alpha, which controls only the level of horizontal smoothing, was set to the default value of 1.

- Error floors of 15% for the apparent resistivity data and 2.2° for the phase were used.

- The inversion algorithm was set to solve for static shifts, but was heavily weighted to force the data to be fit before allowing changes to the static shifts.

- All 2D inversion models completed 200 iterations and were generated on a linear profile oriented perpendicular to the overall geoelectric strike direction (i.e. N45°E; Bertrand et al., 2012). The starting model for each inversion was a 100 Ωm uniform half-space, with a fine mesh that included 86 depth rows and 255 columns. To avoid boundary condition effects, the total model mesh extended 1000 km laterally and 475 km in depth.

The map in Figure 5 identifies which MT measurements were used in each inversion model contained in Figure 6. From the available Contact Energy and GNS Science MT data, only high-quality measurements were included. Also, preference was given to sites located close to the arbitrary 2D profile (white line in Figure 5) that best transects the GNS Science 'deep geothermal' and 'Ohaaki 2008' MT measurements through the centre of the geothermal field. In this way, the Contact Energy and GNS Science MT datasets could be combined to form a single profile with a wide-aperture and a minimal amount of data projection.

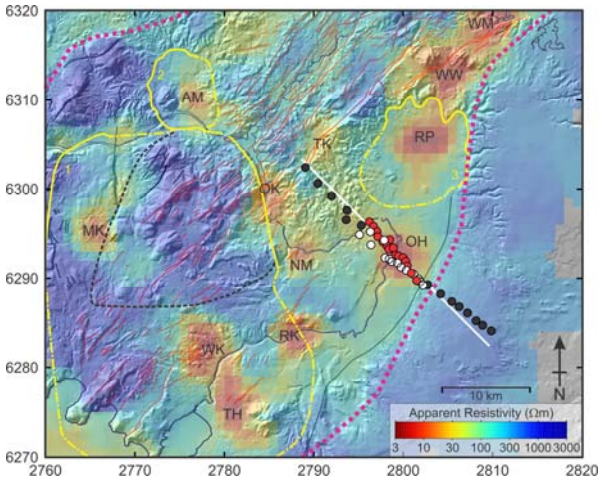

Figure 5: Map showing the location of MT sites used in the 2D inversion modelling study. Red circles show the location of Contact Energy MT measurements; black and white circles denote GNS Science MT measurements. For the inversion of only GNS Science MT data, both black and white sites were used. For the inversion that combines GNS Science and Contact Energy MT data, only the black and red circles were used. The Contact Energy-only inversion used just the red sites. White line shows the 2D inversion profile that is oriented NW-SE and transects the Ohaaki geothermal field.

4. DISCUSSION OF 2D RESISTIVITY MODELS

Comparison of the three inversion models in Figure 6 clearly demonstrates that a wide-aperture (i.e. twice the depth of investigation) is required to image the deep resistivity structure beneath the Ohaaki geothermal field. Further, Figure 6 illustrates that the Contact Energy MT data are capable of resolving the deep resistivity structure, but only when a wide-aperture is used. These conclusions are convincingly realised through the following key observations:

- The only difference between inversion models B and C in Figure 6 is the data used at the Ohaaki geothermal field (model B – Contact Energy MT data; model C - GNS Science MT data). Both inversion models use identical GNS Science data to extend the aperture ~10km NW and SE of the DC resistivity boundaries of the geothermal field.

  These inversion models show remarkable similarity in resistivity structure down to depths of 10 km. Further, the normalised root mean square (rms) data misfit (a measure of the degree of fit of model structure to the measured data) is 1.4 for model B and 1.5 for model C. In essence there is no significant difference between these inversion models. (See Appendix-II for additional discussion of rms data misfit) .

  Therefore, the quality of the Contact Energy MT data is sufficient to image the resistivity structure at depths of 3 – 10 km beneath the Ohaaki geothermal field.

- The only difference between inversion models A and B in Figure 6 is the spatial extent (or aperture) of the MT data used. In model A, only Contact Energy MT data is used which have an aperture of ~8 km. In model B, identical Contact Energy data is used as for model A, but regional GNS Science MT data are added to extend the aperture to ~30 km .

  To a depth of ~4 km (i.e. half the width of the model A aperture), these inversion models show little difference in resistivity structure imaged beneath the Ohaaki geothermal field. However, these models are clearly different at depths of 5 to 10 km. In particular, model A is oscillatory (or rougher) at depth showing a pattern of conductor-resistor-conductor.

  MT inversion models are ill-conditioned and are stabilised (regularised) by seeking smooth or minimum structure models. Smooth models are appropriate since electromagnetic energy propagates diffusively within the Earth, and subsurface structures influence all measurements located within the inductive length-scale for any given period.

  The oscillatory behaviour at depth in model A is an indication that the inversion algorithm is unable (i.e. insufficiently constrained) to generate a spatially smooth model. This observation is quantified by the higher rms misfit of model A (1.8) in comparison to models B (1.4) and C (1.5), which obtain a better data fit with a spatially smoother model. The increased misfit of model A is also seen in Figure 7, which shows the TE mode MT data (black) at a Contact Energy site. The fit to the apparent resistivity data is clearly improved at long-periods for the inversion that includes GNS Science data (red dots) compared to the model that used only Contact Energy data (blue dots).

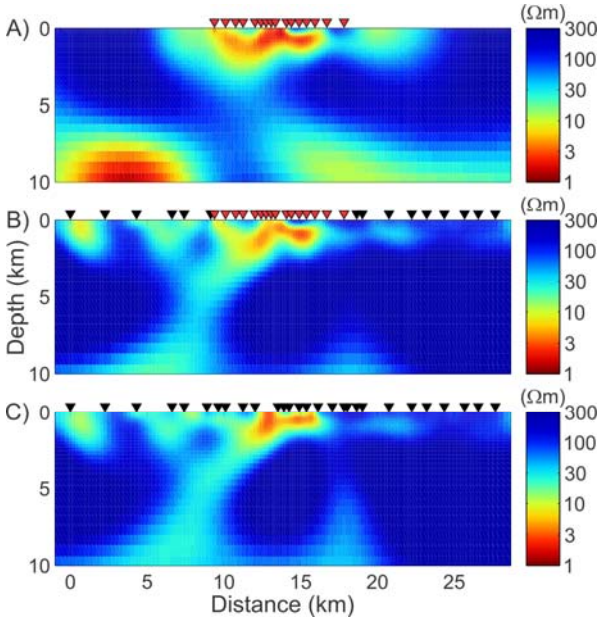

Figure 6: 2D resistivity inversion models of the TE and TM mode MT impedance data projected onto the profile shown by the white line in Figure 5. These inversion models were computed using: A) Contact Energy-only MT data (red triangles), B) Contact Energy (red triangles) and GNS Science (black triangles) MT data, and C) GNS Science-only MT data (black triangles). All inversion models were generated using identical control settings and starting models. The locations of the MT sites used in each inversion model are shown in Figure 5.

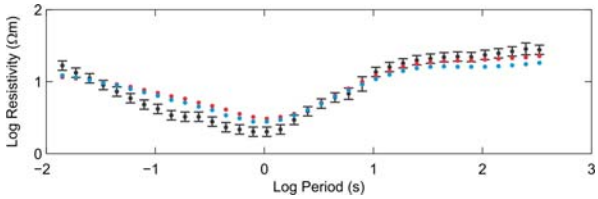

Figure 7: TE mode MT data (black dots) at a Contact Energy MT site, and the model fit for the Contact Energy only inversion (blue dots) and the inversion that combined GNS Science and Contact Energy data (red dots).

This comparison shows that without the wider data coverage provided by the GNS Science MT data, the Contact Energy MT data alone cannot reliably resolve the resistivity structure beneath the Ohaaki geothermal field beyond ~4 km depth, or as a rule of thumb, to a depth greater than half the aperture.

CONCLUSION

A series of 2D inversions were generated to study data characteristics and aspects of survey design required to image the resistivity structure beneath the Ohaaki geothermal field at depths of 3 – 10 km. These inversion models clearly show that only when regional GNS Science MT data are added to the Contact Energy MT data is the resistivity structure at these depths resolved.

This study has illustrated that MT surveys should include measurements that cover a spatial extent that is at least twice the intended depth of investigation. However, note that this guideline is simply a 'rule-of-thumb' and it is imperative to also remember that the depth penetration of MT fields is highly dependent on the conductivity structure of the Earth. Like all rules of thumb, this is an approximate guide.

ACKNOWLEDGEMENTS

Cooperation from Contact Energy and landowners in the survey area is greatly appreciated. This project was funded by public research funding from the government of New Zealand and Contact Energy.

REFERENCES

Bertrand, E.A., Caldwell, T.G., Hill, G.J., Wallin, E.L., Bennie, S.L., Cozens, N., Onacha, S.A., Ryan, G.A., Walter, C., Zaino, A., Wameyo, P.: Magnetotelluric imaging of upper-crustal convection plumes beneath the Taupo Volcanic Zone, New Zealand, *Geophysical Research Letters*, 39(2), L02304, doi:10.1029/2011GL050177 (2012).

Bibby, H.M., Caldwell, T.G., Davey, F.J., Webb, T.H.: Geophysical evidence on the structure of the Taupo Volcanic Zone and its hydrothermal circulation, *Journal of Volcanology and Geothermal Research*, 68, 29-58 (1995).

Caldwell, T.G., Bibby, H.M., Brown, C.: The magnetotelluric phase tensor, *Geophysical Journal International, 158*, 457-469 (2004).

Henrys, S.A., van Dijck, M.F.: Structure of concealed rhyolites and dacites in the Broadlands-Ohaaki geothermal field, Proceedings of the 9th New Zealand Geothermal Workshop, Auckland, New Zealand (1987).

Hochstein M.P., and Hunt, T.M.: Seismic, gravity and magnetic studies, Broadlands geothermal field, New Zealand, *Geothermics Special Issue* 2, 333-346 (1970).

Hunt, T.M.: Geophysical exploration of the Broadlands Ohaaki) geothermal field: Review, *Proceedings of the 11th New Zealand Geothermal Workshop*, Auckland, New Zealand (1989).

Ingham, M.: Audiomagnetotelluric/Magnetotelluric soundings of the Broadlands-Ohaaki geothermal field, Proceedings of the 11th New Zealand Geothermal Workshop, Auckland, New Zealand (1989).

Risk, G.F., Macdonald, W.J.P., Dawson, G.B.: DC resistivity surveys of the Broadlands geothermal region, *New Zealand*, *Geothermal Special Issue*, 2, 287-294 (1970).

Risk, G.F., Groth, M.J., Rayner, H.H., Dawson, G.B., Bibby, H.M., Macdonald, W.J.P., Hewson, C.A.Y.: The resistivity boundary of the Broadlands geothermal field, *Geophysics Division Technical Report No 123*, 42p, Department of Scientific and Industrial Research, Wellington, New Zealand (1977).

Risk, G.F.: Induced polarization IP) in the Broadlands geothermal field, Proceedings of the 3rd New Zealand Geothermal Workshop, Auckland, New Zealand (1981).

Rodi, W., and Mackie, R.L.: Nonlinear conjugate gradients algorithm for 2-D Magnetotelluric inversion, *Geophysics*, 66, 174-187 (2001).

Risk, G.F.: Resurvey of the resistivity boundary of Ohaaki geothermal field, 1975-1992, Proceedings of the 15th New Zealand Geothermal Workshop, Auckland, New Zealand (1993).

Simpson, F. and Bahr, K.: Practical Magnetotellurics: Cambridge University Press, Cambridge, 254 p, (2005).

Sinclair Knight Merz (SKM): Ohaaki geothermal field, MT survey summary, 10 p, ZP00590-RPT-GS-005 (2011).

Wilson, C.J.N., Houghton, B.F., McWilliams, M.O., Lanphere, M.A., Weaver, S.D., Briggs, R.M.: Volcanic and structural evolution of Taupo Volcanic Zone, New Zealand: a review, *Journal of Volcanology and Geothermal Research*, 68, 1-28 (1995).

APPENDIX – I: MT SOURCE FIELDS

The MT method requires measurements of the time variations of electric and magnetic fields at the surface of the Earth, that are made in the presence of the Earth's internal magnetic field (which is virtually constant at the frequencies of interest in MT). Therefore, it is the external magnetic fields, which are generated by two mechanisms that operate within distinct frequency regimes that comprise the source for MT measurements. At f > ~1 Hz (or at periods shorter than ~1 s), signals originate from worldwide lightning activity and traverse the globe within a leaky waveguide bounded by the Earth and ionosphere (which are conductive in comparison to the atmosphere). At frequencies < ~1 Hz (or periods greater than ~1 s) the MT signal originates from interactions between the Earth's magnetosphere and the solar wind. Temporal changes in the solar wind due to sunspot activity and other phenomena on the sun excite harmonics of the Earth's magnetosphere and induce large-scale electric currents in the ionosphere. These induced currents cause variations in the magnetic field that can be measured at the surface of the Earth.

Solar activity undergoes an 11 year cycle that is sometimes referred to as the 'sunspot cycle'. At the maximum of the solar cycle, hundreds of sunspots may be present at any one time. In contrast, during the solar minimum, sunspots are rare (Figure A1). The solar cycle thus directly influences the strength of the natural MT source fields at periods greater than 1 s. Specifically, the likelihood of encountering a period of strong signal is lower during the solar minimum than during the solar maximum, and in areas with high-levels of man-made noise, this cycle can significantly influence MT data quality.

The so-called 'dead-band' (Figure A2) occurs in the frequency range 0.5 – 5 Hz (or periods of 0.2 – 2 s) between the two mechanisms that generate the external fields exploited by MT measurements (Simpson and Bahr, 2005). In other words, low-amplitude signals in this band are a result of one source mechanism effective above ~1 Hz, and the other effective below ~1 Hz. This band of low signal strength combined with the frequency response and noise characteristics of the magnetic field sensors often results in reduced MT data quality between the period range ~1 - 10 s.

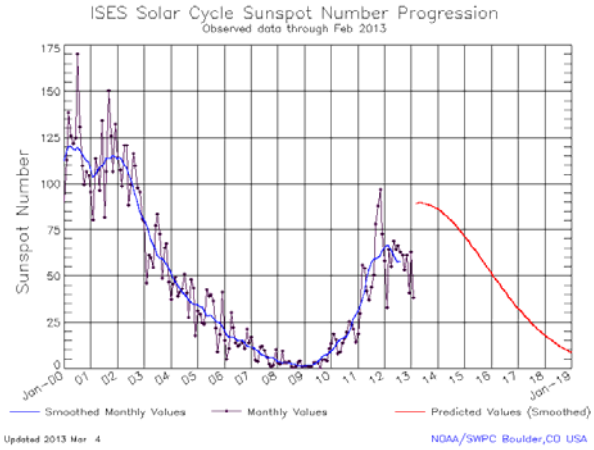

Figure A1: Sunspots (smoothed with monthly values). http://www.solarham.net/trends.htm.

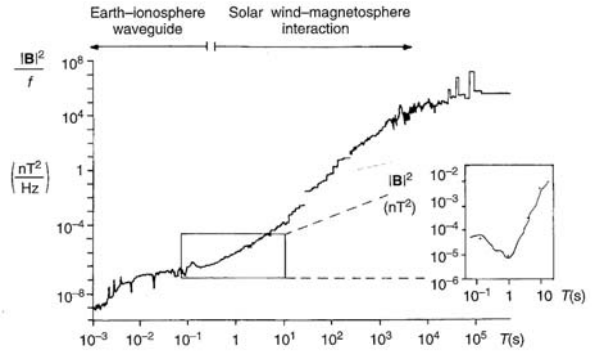

Figure A2: Power spectrum of natural MT signals plotted as a function of period (T) showing '1/f characteristics'. For T>~1 s, interaction between the solar wind and the Earth's magnetosphere generate a time-varying magnetic field that is incident on the Earth's surface. For T<~1 s, worldwide lightning activity generate the source fields measured by MT instruments. The inset shows the reduced signal power ($|B|^2$) in the 'dead-band'. Figure reproduced from Simpson and Bahr, 2005.

APPENDIX - II: RMS DATA MISFIT

The normalized root-mean-square (rms) data misfit quantifies the fit of an inversion model to the measured data and is calculated using the formula:

$$\Phi_{rms} = \sqrt{\frac{1}{N}\left[\sum_{i=1}^{i=N}\left(\frac{\rho_i - m_i}{e_i}\right)^2\right]}$$

where N represents the number of data points,

ρ_i represents the apparent resistivity data,

m_i represents the model response, and

ei represents the data error.

In MT, smooth inversion models are sought that also fit the measured MT data to within an acceptable level. However, these are opposing requirements and the balance between them is controlled by the regularization parameter τ. Low values of τ will result in a rough model that gives a small rms misfit, while high values of τ will yield a spatially smooth model, but with a high rms misfit. Ideally, rms misfit values should be in the range 1 to 1.5. RMS misfit values lower than 1 indicates an over-fitting of the measured data, which also includes noise. In contrast, rms misfit values greater than ~1.5 can indicate that the model is not honouring the measured data. Note however, that error floors applied to the measured data also influence the normalized rms misfit calculation (by increasing the value of e_i) and therefore simply judging an inversion model based solely on an rms misfit value can be misleading.